crystals

MDPI

Article

Packing Motifs in $[M(bpy)_2X_2]$ Coordination Compounds (bpy = 2,2′-bipyridine; X = F, Cl, Br, I)

Edwin C. Constable and Catherine E. Housecroft *

Department of Chemistry, University of Basel, BPR 1096, Mattenstrasse 22, Postfach, 4002 Basel, Switzerland
* Correspondence: catherine.housecroft@unibas.ch

Abstract: Packing motifs within structurally characterized *cis*-$[M(bpy)_2X_2]$ (M = any metal, bpy = 2,2′-bipyridine, X = F, Cl, Br, I) coordination compounds have been investigated using data from the Cambridge Structural Database. Compounds fall into two classes: non-solvated *cis*-$[M(bpy)_2X_2]$ moieties and those with additional lattice molecules (solvent or other molecules). A recurring packing motif is a dimeric unit involving intermolecular face-to-face π-stacking of bpy ligands and CH_{bpy}...X contacts, although in several cases, slippage of the stacked bpy units reduces the effectiveness of the face-to-face interaction leaving the CH_{bpy}...X contacts as the dominant crystal-packing interaction. The prevalence of the dimeric unit versus the assembly of 1D-chains in the solid state is described.

Keywords: metal complexes; 2,2′-bipyridine; *cis*-$[M(bpy)_2X_2]$; π-stacking; C–H...X contacts

check for updates

Citation: Constable, E.C.; Housecroft, C.E. Packing Motifs in $[M(bpy)_2X_2]$ Coordination Compounds (bpy = 2,2′-bipyridine; X = F, Cl, Br, I). *Crystals* **2023**, *13*, 505. https://doi.org/10.3390/cryst13030505

Academic Editor: Josefina Perles

Received: 27 February 2023
Revised: 7 March 2023
Accepted: 12 March 2023
Published: 15 March 2023

1. Introduction

The structural information in the Cambridge Structural Database [1] allows the detailed analysis of structural patterns at the molecular level, as well as in terms of crystal packing. We have recently drawn attention to a dominant crystal-packing motif in the solid-state structures of $[M(bpy)_3]^{q+}$ salts (bpy = 2,2′-bipyridine) containing halide anions, in which six homochiral $[M(bpy)_3]^{q+}$ cations embrace a halide anion (Figure 1a) [2]. We subsequently extended this investigation to $[M(bpy)_3]^{q+}$ salts containing $[XY_3]^{m-}$ and $[XY_4]^{m-}$ anions, and demonstrated that four packing motifs dominate, the most common of which involve a hexagonal arrangement of six cations with anions either in the center or lying above and/or below the centroid of the hexagon (Figure 1b) [3]. Homochiral layers of $[M(bpy)_3]^{q+}$ cations are common in the crystal packing of these structures. In these first two studies, we showed that short contacts between an anion and atoms H3 and H3′ of the bpy ligands (see Scheme 1 for numbering) are often supplemented by contacts with H4 and H5. This leads to a more general theme in the supramolecular chemistry of crystals containing $[M(bpy)_3]^{q+}$ cations [3]. The chirality of the $[M(bpy)_3]^{q+}$ cation is fundamental to the packing interactions that we have described [2,3], and we decided, therefore, to extend the structural investigations to neutral *cis*-$[M(bpy)_2X_2]$ compounds in which X = F, Cl, Br, and I. The presence of intermolecular face-to-face π-stacking interactions between bpy domains has been noted by a number of authors [4–15], and Kruszynski and coworker recognized the interactions depicted in Scheme 2 in $[Cd(bpy)_2F_2]\cdot3.5H_2O$ and $[Cd(bpy)_2I_2]$, respectively [6]. Intermolecular CH_{bpy}...X contacts in *cis*-$[M(bpy)_2X_2]$ complexes have also been described [7,10,16–18]. However, the recurrence of particular packing motifs within the wide range of structurally characterized *cis*-$[M(bpy)_2X_2]$ species and the relationship between them has not, to the best of our knowledge, been addressed.

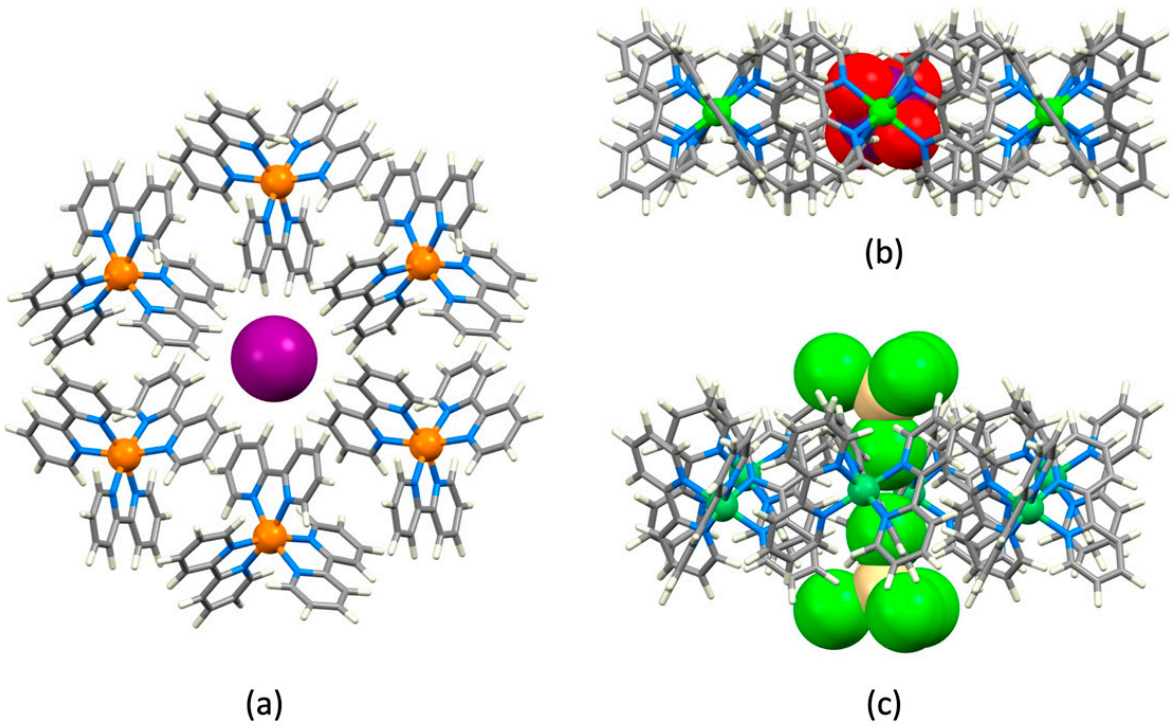

Figure 1. Hexagonal motifs in (**a**) $[Li(bpy)_3]I{\cdot}bpy$ (CSD refcode REXVOF) [19], (**b**) $[Zn(bpy)_3]$-$[CrO_4]_{0.5}[NO_3]{\cdot}6.5H_2O$ (refcode XUJDEL) [20], and (**c**) $[Ni(bpy)_3][CdCl_4]$ (refcode BINZON) [21]. Color code: C, gray; H, off-white; N, blue; I, purple; Cl, green; O, red.

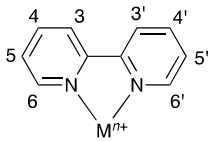

Scheme 1. Hydrogen atom numbering in 2,2′-bipyridine; the conformation adopted by the metal-coordinated chelating ligand is shown.

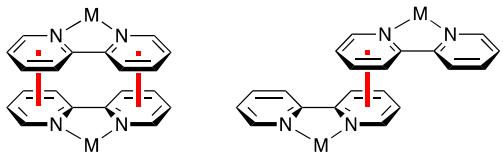

Scheme 2. Two bpy...bpy stacking interactions described by Kruszynski in $[Cd(bpy)_2F_2]{\cdot}3.5H_2O$ and $[Cd(bpy)_2I_2]$, respectively [6].

2. Methods

Conquest (version 2022.3.0 including November 2022 updates) [22] was used to search the CSD [1] for the $[M(bpy)_2X_2]$ unit (M = any metal; X = halogen) and neutral compounds were selected from the hits that included both neutral and cationic species. Substituted bpy ligands were excluded by explicitly entering C-bonded H atoms. The connectivity of M was restricted to six, and no restriction was placed on the isomer (*cis* or *trans*). The connectivity of each X atom was constrained to one, and M–X bonds, as well as the inter-ring C–C bond in bpy, were set to 'any type'. Polymeric structures were excluded.

Analysis of structures was carried out using Mercury (version 2022.3.0) [23]. In some structures, H atom coordinates were not available, and in this case, the H positions were added in Mercury [23]. All H positions were normalized within Mercury, such that all C–H bond lengths were 1.089 Å. The settings in Mercury for a 'short contact' (sum of the van der Waals radii + 0.1 Å) were applied to locate H...X interactions, as well as cation...anion contacts. Disordered structures were retained in the analysis.

3. Initial Search Results and Selection of Structures for Detailed Analysis

An initial search of the CSD (version 2.22.3.0) [22] for the $[M(bpy)_2X_2]$ unit gave 86 hits. Of these, two were *trans*-isomers (CSD refcodes HIQPIH and NEZTEU). Of interest here is the fact that *trans*-$[Ru(bpy)_2Br_2]Br$ (refcode NEZTEU [24]) contains motifs comprising a bromide ion surrounded by four *trans*-$[Ru(bpy)_2Br_2]^+$ cations with short H3 and H3′ to Br^- contacts from two bpy ligands supplemented by contacts to H5 and H6 of two other bpy ligands (Figure 2 and Table 1). This packing motif was not discussed in the original work [24], and is complementary to the halide-embraces that we described for halide salts of $[M(bpy)_3]^{q+}$ (Figure 1a) [2]. Figure 2 illustrates the bromide embrace in *trans*-$[Ru(bpy)_2Br_2]Br$ and also shows that this motif is supported by additional CH_{bpy}...Br–Ru interactions involving bpy atoms H4 and H4′ (CH_{bpy}...Br distances = 2.697 and 2.738 Å, C_{bpy}...Br = 3.626(6) and 3.664(5) Å, ∠C–H...Br = 142.7 and 142.9°).

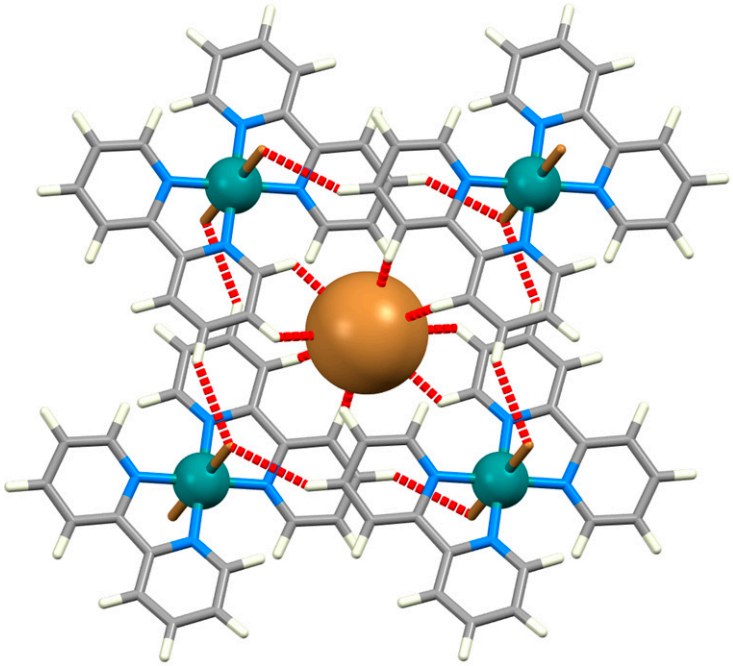

Figure 2. Bromide embrace motif in *trans*-$[Ru(bpy)_2Br_2]Br$ (refcode NEZTEU) [24] showing eight H3...Br^-, H3′...Br^-, H5...Br^-, and H6...Br^- contacts and eight RuBr...H4 and RuBr...H4′ interactions.

Table 1. Parameters for CH_{bpy}...Br^- ion contacts in *trans*-$[Ru(bpy)_2Br_2]Br$.

REFCODE Space Group	Range CH...Br/Å (Mean CH...Br/Å)	Range C...Br/Å (Mean C...Br/Å)	Range ∠C–H...Br/° (Mean ∠C–H...Br/°)	Ref
NEZTEU $P\bar{1}$	2.851–3.080 (2.995)	3.701–3.779 (3.743)	120.9–134.8 (126.5)	[24]

For five structures in the initial search, atom coordinates were unavailable (refcodes QQQEQD, QQQEQG, QQQEQJ, QQQEQM, and QQQEQP). The structures with CSD refcodes YEYJAQ, YEYLIA, YEYLAS, YEYJUK, YEYKEV, YEYKAR, YEYKUL, ESIXOU, and ESILOH contained additional molecular species, which significantly impacted the crystal packing. These were excluded from the detailed analysis. This left 70 structures (including several redeterminations) that fell into the classes of non-solvated *cis*-[M(bpy)$_2$X$_2$], *cis*-[M(bpy)$_2$X$_2$] with lattice molecules (solvent or other molecules), and salts of *cis*-[M(bpy)$_2$X$_2$]$^{q+}$. In this paper, we focus only on the neutral *cis*-[M(bpy)$_2$X$_2$] compounds. We note that data for Kruszynski's structural determination of [Cd(bpy)$_2$I$_2$] mentioned in the introduction [6] are not available in the CSD. However, this polymorph is isostructural with the entry TIBLAT and so is included in our analysis.

4. Non-Solvated *cis*-[M(bpy)$_2$X$_2$] Compounds

Non-solvated *cis*-[M(bpy)$_2$X$_2$] complexes fall into several structural groups, but typically they exhibit a common packing motif. Compounds in the first group (Table 2) crystallize in the monoclinic space group $P2_1/c$; the two bpy ligands are crystallographically independent, as are the two halido ligands. The packing motifs in the first group are centrosymmetric dimers associated through face-to-face π-stacking of pyridine rings and CH...X contacts. The two independent bpy ligands are labelled A and B in Figure 3, and the two dimeric motifs are shown in Figure 3a, b, and c, respectively. The dimeric motif involving a bpy$_A$...bpy$_A$ π-stacking interaction involves both pyridine rings (Figure 3a,b), whereas the bpy$_B$...bpy$_B$ π-stacking contact is offset such that only one pyridine ring of each bpy is involved (Figure 3c). Centroid...centroid distances are given in Table 2 and are consistent with the ranges quoted by Janiak [25]. Each stacking interaction is supported by weak CH...X contacts involving H3 (Figure 3a,b) or H4 (Figure 3c), and metric parameters for the interactions are given in Table 2. The two motifs combine to generate 1D-chains as shown in Figure 3d, and the chains are interconnected by additional CH...Br interactions involving bpy H4 and H5 atoms. The data in Table 2 illustrate that on going from X = Cl to Br to I, the centroid...centroid distances for the π-stacking interactions increase, leading to a decrease in the efficiency of the interactions. This is especially noticeable in *cis*-[Mn(bpy)$_2$I$_2$] (CSD refcode ISAFOY [26]). However, it is noteworthy that the packing motif persists despite the reduced effectiveness of the face-to-face π-stacking. Significantly, one polymorph of *cis*-[Cd(bpy)$_2$I$_2$] (CSD refcode TIBLAT [27]) crystallizes in the orthorhombic space group *Pbcn* with half a molecule in the asymmetric unit; all bpy ligands (and all iodido ligands) are, therefore, crystallographically equivalent. Figure 4a and Table 3 demonstrate that efficient face-to-face π-stacking is restored and, again, the interaction is augmented by CH...X contacts involving H3 and H4. The unit is repeated along the crystallographic *c*-axis, giving 1D-chains (Figure 4b). The iodido complex *cis*-[Ca(bpy)$_2$I$_2$] (CSD refcode TAQQET [28]) adopts the same structure (Table 3).

Table 2. Metric parameters for the face-to-face π-stacking and CH...X contacts in the centrosymmetric dimeric motifs in the first group of non-solvated *cis*-[M(bpy)$_2$X$_2$].

REFCODE Space Group	M	X	Centroid... Centroid (Figure 3a,b)/Å	Centroid... Centroid (Figure 3c)/Å	CH...X, C...X (Figure 3a,b)/Å	∠C–H...X (Figure 3a,b)/°	CH...X, C...X (Figure 3c)/Å	∠C–H...X (Figure 3c)/°	Ref
GALMAH $P2_1/c$	Mn	Cl	3.92	3.66	2.705, 3.639(5)	143.5	2.669, 3.650(5)	149.7	[16]
GALMAH01 $P2_1/c$	Mn	Cl	3.85	3.64	2.630, 3.587(3)	146.4	2.670, 3.618(3)	145.1	[18]
IRUBAB $P2_1/c$	Co	Cl	3.93	3.64	2.660, 3.648(2)	150.5	2.662, 3.619(2)	146.3	[29]
WABWAZ $P2_1/c$	Cd	Cl	3.91	3.70	2.699, 3.635(7)	143.8	2.700, 3.654(7)	146.0	[30]
DEYQUU01 $P2_1/c$	Cd	Br	4.06	3.84	2.814, 3.710(6)	139.5	2.826, 3.748(6)	142.4	[31]
TIRCON $P2_1/c$	Mn	Br	4.07	3.76	2.746, 3.673(3)	142.8	2.760, 3.692(3)	143.5	[8]
TIRCON02 $P2_1/c$	Mn	Br	4.05	3.75	2.713, 3.630(2)	141.6	2.758, 3.655(2)	139.6	[32]
UPUTIJ $P2_1/c$	Co	Br	4.14	3.77	2.751, 3.718(6)	147.8	2.751, 3.700(6)	145.4	[33]
UPUTIJ01 $P2_1/c$	Co	Br	4.07	3.75	2.704, 3.664(3)	146.7	2.731, 3.648(3)	141.7	[34]
ISAFOY $P2_1/c$	Mn	I	4.39	4.06	2.966, 3.820(6)	135.5	2.985, 3.848(6)	136.4	[26]

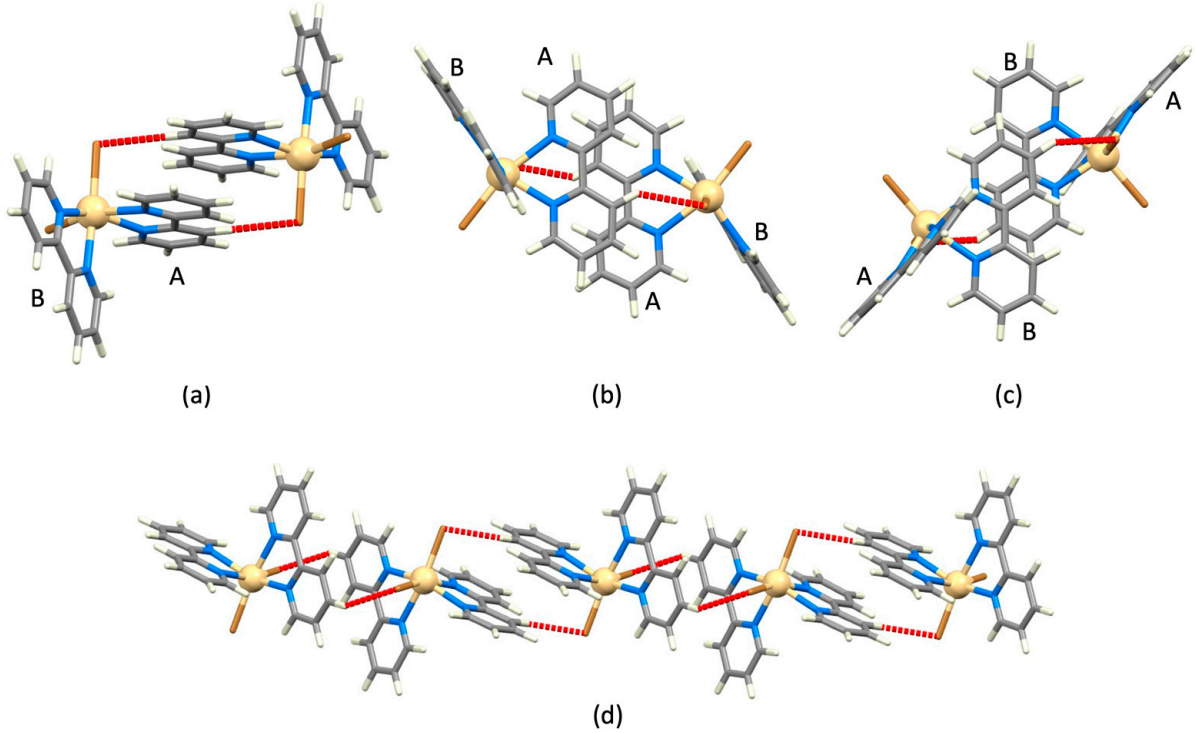

Figure 3. Primary packing motifs in the first group of non-solvated *cis*-[M(bpy)$_2$X$_2$] illustrated with the structure of *cis*-[Cd(bpy)$_2$Br$_2$] (CSD refcode DEYQUU01 [31]). (**a**,**b**) Two views of the centrosymmetric bpy$_A$...bpy$_A$ π-stacking interaction with H3...Br contacts (in red), (**c**) the centrosymmetric bpy$_B$...bpy$_B$ π-stacking interaction with H3...Br contacts (in red), and (**d**) heterochiral 1D-chains resulting from a combination of the two motifs.

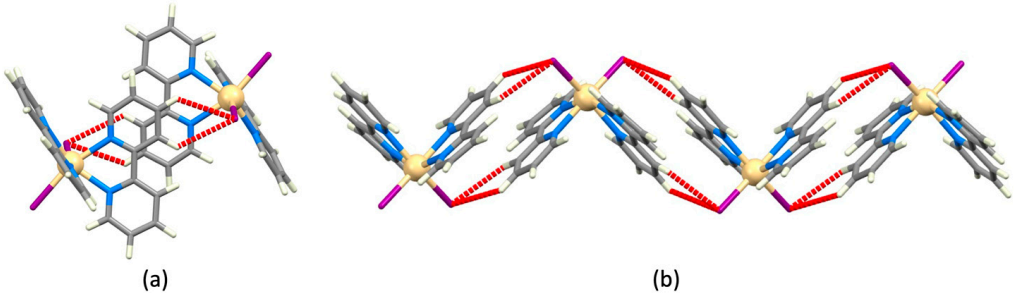

Figure 4. Packing interactions in *cis*-[Cd(bpy)$_2$I$_2$] (CSD refcode TIBLAT [27]): (**a**) π-stacking interaction with H3...I and H4...I contacts (in red), and (**b**) assembly of a 1D-chain.

Table 3. Metric parameters for the face-to-face π-stacking and CH...X contacts in the packing motif in *cis*-[M(bpy)$_2$I$_2$] (M = Cd, Ca). See Figure 4a.

REFCODE Space Group	M	X	Centroid...Centroid/Å	CH...I; C...I/Å	∠C–H...I/°	Ref
TIBLAT *Pbcn*	Cd	I	3.94	3.200, 3.247; 3.950(5), 3.979(3)	126.8, 125.5	[27]
TAQQEH *Pnca*	Ca	I	3.83	3.220, 3.255; 3.970(7), 3.991(6)	126.9, 125.8	[28]

We noted earlier that the structure of *cis*-[Mn(bpy)$_2$I$_2$] (CSD refcode ISAFOY [26], Table 2) exhibits non-optimal face-to-face π-stacking. It is, therefore, significant that a second polymorph (CSD refcode ISAFOY01 [14]) has been reported, and that this is structurally analogous to *cis*-[Cd(bpy)$_2$I$_2$] (CSD refcode ABEBIV [35], a polymorph of the compound with CSD refcode TIBLAT, Figure 4). These polymorphs of *cis*-[Mn(bpy)$_2$I$_2$] and *cis*-[Cd(bpy)$_2$I$_2$] crystallize in the monoclinic space group *C*2/*c* and exhibit a packing motif reminiscent of that shown in Figure 3c. However, whereas the latter is centrosymmetric, that shown in Figure 5a contains stacked bpy units that are related by a glide plane. Parameters for the face-to-face π-stacking and CH...X contacts in this motif are given in Table 4. Since each motif contains two crystallographically independent bpy ligands, all bpy...bpy stacking interactions within the structure are equivalent; the motifs pack into heterochiral sheets (Figure 5b) supported by the interactions detailed in Table 4 and additional CH...I contacts.

Table 4. Metric parameters for the face-to-face π-stacking and CH...X contacts in the motif in *cis*-[M(bpy)$_2$I$_2$] (M = Mn, Cd). See Figure 5a.

REFCODE Space Group	M	X	Centroid...Centroid/Å	CH...X; C...X/Å	∠C–H...X/°	Ref
ISAFOY01 *C*2/*c*	Mn	I	3.91	3.007, 2.985; 3.930(9), 3.918(9)	142.9, 143.9	[14]
ABEBIV *C*2/*c*	Cd	I	3.92	3.012, 3.037; 3.967(8), 3.982(8)	146.6, 145.4	[35]

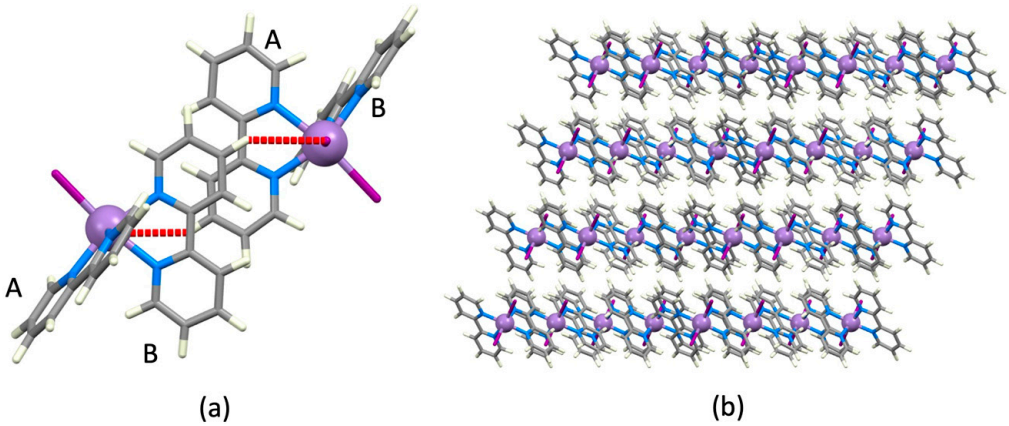

Figure 5. Packing interactions in *cis*-[Mn(bpy)$_2$I$_2$] (CSD refcode ISAFOY01 [14]): (**a**) the basic motif contains a π-stacking interaction and H4...I contacts (in red), and (**b**) assembly of heterochiral layers. The crystallographically independent bpy ligands are labelled A and B.

A second polymorph of each of *cis*-[Mn(bpy)$_2$Br$_2$] (CSD refcodes TIRCON/TIRCON02 in Table 2 and TIRCON01 in Table 5) and *cis*-[Cd(bpy)$_2$Br$_2$] (CSD refcode DEYQUU01 in Table 2, and DEYQUU and TIBLIB in Table 5) has also been structurally characterized and this structure type represents an alternative packing of non-solvated *cis*-[M(bpy)$_2$Br$_2$] molecules (Table 5) in which bpy...bpy π-stacking is absent. The dominant crystal-packing interactions involve H3...Br and H5...Br contacts (Table 5). To allow a comparison with the first group of *cis*-[Mn(bpy)$_2$Br$_2$] compounds described above, the packing motifs in the second group are best considered as shown in Figure 6. A centrosymmetric motif involving H5...Br contacts (Figure 6a,b) is related to that shown in Figure 3c. However, the motif in Figure 6b is slipped with respect to that in Figure 3c. This is a consequence of a change from an H4...Br to H5...Br interaction and it results in loss of an effective bpy...bpy π-stacking interaction; in *cis*-[Mn(bpy)$_2$Br$_2$] (Figure 6b), the distance between the centroids of the central two pyridine rings is 4.47 Å, which is at the upper limit considered by Janiak [25]. Additional H5...Br contacts link the motifs into heterochiral 1D-chains (Figure 6c), and these are interconnected through H3...Br and CH...π interactions [36] (Figure 6d).

Table 5. Metric parameters for CH...X contacts in the group of non-solvated *cis*-[M(bpy)$_2$X$_2$] (Figure 6). H3 and H5 in the columns headings refer to bpy H atoms.

REFCODE Space Group	M	X	CH3...X, C...X/Å	∠C–H3...X/°	CH5...X; C...X/Å	∠C–H5...X/°	Ref
TIRCON01 *C*2/*c*	Mn	Br	2.937, 3.596(5)	119.2	3.006, 2.835; 3.722(5), 3.795(4)	123.7, 147.1	[37]
TIBLIB [a] *C*2/*c*	Cd	Br	2.959, 3.613(7)	118.9	3.007, 2.865; 3.728(7), 3.829(6)	124.0, 147.6	[27]
DEYQUU *C*2/*c*	Cd	Br	2.964, 3.612(5)	118.4	3.023, 2.865; 3.737(4), 3.838(3)	123.6, 147.5	[38]

[a] TIBLIB has recently (2023) been updated to DEYQUU02 in the CSD.

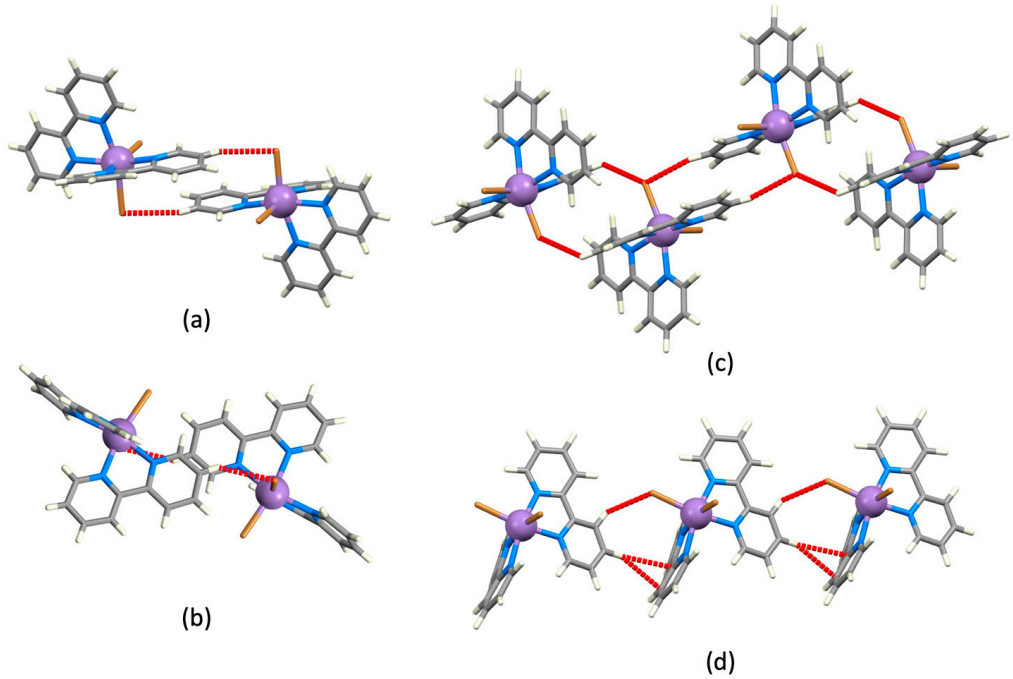

Figure 6. (**a**,**b**) Two views of the centrosymmetric motif in *cis*-[Mn(bpy)$_2$Br$_2$] (CSD refcode TIRCON01 [37]) involving H5...Br contacts, and (**c**) propagation of chains supported by H5...Br contacts. (**d**) Chains are interconnected through H3...Br and CH...π interactions.

5. *cis*-[M(bpy)$_2$X$_2$] Compounds with Lattice Molecules

The analysis in Section 4 of the crystal structures of non-solvated *cis*-[M(bpy)$_2$X$_2$] complexes with X = Cl, Br, and I demonstrates the dominance of a dimeric motif featuring a bpy...bpy π-stacking interaction augmented by CH$_{bpy}$...X interactions (H$_{bpy}$ = H3, H4 or H5). In only a few cases was this motif absent. We now move from non-solvated *cis*-[M(bpy)$_2$X$_2$] to structures containing solvent or other molecules in the crystal lattice starting with hydrates. The compounds *cis*-[Co(bpy)$_2$Cl$_2$]·2H$_2$O (CSD refcode NAPBIT) [39], *cis*-[Co(bpy)$_2$Cl$_2$]·3H$_2$O (CSD refcode UNOJEN) [40], *cis*-[Mn(bpy)$_2$Cl$_2$]·2H$_2$O·EtOH (CSD refcode SASQAE) [5], *cis*-[Ni(bpy)$_2$Cl$_2$]·2H$_2$O·0.5MeCN (CSD refcode CEFHIE) [13], and *cis*-[Ru(bpy)$_2$Cl$_2$]·3.5H$_2$O (CSD refcode DOGMOB [4]) crystallize in the monoclinic space group *C*2/*c* with half of one [M(bpy)$_2$X$_2$] unit in the asymmetric unit. The centrosymmetric motif shown in Figure 7a is common to these structures (Table 6) and the CH$_{bpy}$...X interactions involve H3 and H3′. Extension of the interactions depicted in Figure 7a leads to the assembly of 1D-chains (Figure 7b). Note the relationship between this structure and that shown for one polymorph of *cis*-[Cd(bpy)$_2$I$_2$] (Figure 4b).

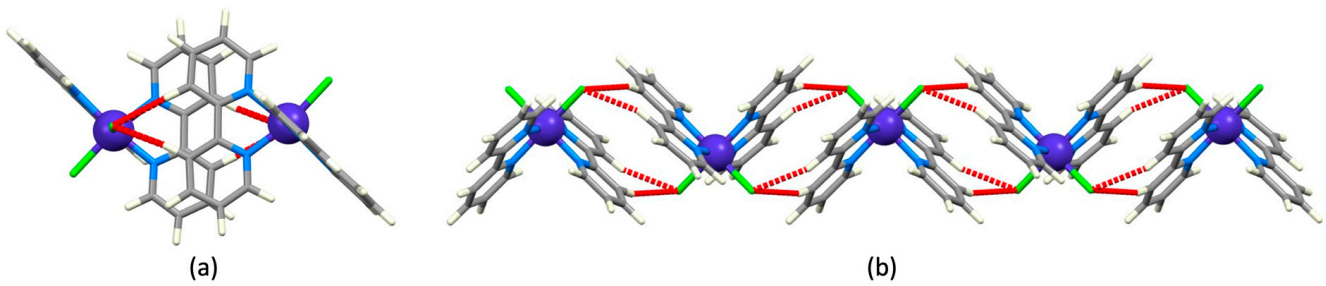

Figure 7. Packing interactions in *cis*-[Co(bpy)$_2$Cl$_2$] (CSD refcode NAPBIT [39]): (**a**) centrosymmetric π-stacking interaction between bpy ligands with supporting H3...Cl and H3′...Cl contacts (in red), and (**b**) assembly of a 1D-chain.

Table 6. Metric parameters for the bpy...bpy π-stacking and CH_{bpy}...X interactions in *cis*-$[Co(bpy)_2Cl_2]\cdot 2H_2O$ (see Figure 7) and related compounds.

REFCODE Space Group	M	X	Centroid...Centroid/Å	CH...X; C...X/Å	∠C–H...X/°	Ref
SASQAE $C2/c$	Mn	Cl	3.79	2.639, 2.676; 3.671(5), 3.730(3)	157.9, 162.8	[5]
NAPBIT $C2/c$	Co	Cl	3.92	2.623, 2.703; 3.643(3), 3.750(2)	155.7, 161.2	[39]
UNOJEN $C2/c$	Co	Cl	3.89	2.663, 2.707; 3.683(6), 3.757(3)	155.7, 161.7	[40]
CEFHIE $C2/c$	Ni	Cl	3.92	2.682, 2.757; 3.704(4), 3.788(3)	156.0, 157.8	[13]
DOGMOB $C2/c$	Ru	Cl	3.94	2.723, 2.795; 3.705(5), 3.823(4)	149.8, 157.3	[4]
BAYCEN $C2/c$	Ru	Cl	4.07	2.763, 2.918; 3.818(3), 3.948(3)	157.9; 163.0	[41]
OCERUK $C2/c$	Ru	Cl	4.17	2.817; 3.729(9) [b]	141.3 [b]	[42]
DUYWEZ $P2_1/n$	Co	Cl	3.83	2.608, 2.798; 3.64(1), 3.85(1)	157.5, 162.7	[43]
NIGTEF $C2/c$	Ni	Br	3.90, 4.17	2.797, 2.842, 2.670; 3.842(3), 3.882(3), 3.558(3) [c]	159.7, 160.8, 138.4 [c]	[44]
XURZOZ $P\bar{1}$	Mn	Cl	3.76, 3.85	2.789, 2.854, 2.550, 2.707; 3.810(5), 3.824(6), 3.559(4), 3.791(6)	156.1, 148.4, 153.7, 173.4	[11]
AZAQUO $P\bar{1}$	Ru	Cl	4.12, 4.37	2.627, 2.658, 2.896, 2.998; 3.68(2), 3.70(2), 3.67(2), 3.63(2)	159.4, 161.5, 120.6, 124.6	[45]
KESYEP [a] $P\bar{1}$	Ru	Cl	3.98, 4.02	2.761, 2.724, 2.594, 3.198; 3.825(4), 3.788(4), 3.559(5), 4.243(4)	165.5, 165.5, 147.2, 161.1	[46]
JEMKEU $P\bar{1}$	Ru	Cl	3.98, 4.01	2.768, 2.728, 2.601, 3.200; 3.834(3), 3.794(3), 3.566(4), 4.245(4)	166.1, 166.2, 147.3, 161.1	[47]
ABUWAV $Pbca$	Ni	Cl	3.87	2.503, 2.807; 3.545(5), 3.861(4)	159.8, 162.9	[48]
CIBJIJ $Pbca$	Os	Cl	3.97	2.578, 2.838; 3.61(1), 3.88(1)	157.7, 160.1	[49]

[a] KESYEP has recently (2023) been updated to JEMKEU01 in the CSD. [b] The H3′...Cl contact (3.614 Å) is too long to be considered. [c] One H3′...Br contact (3.535 Å) is too long to be considered.

The lower part of Table 6 (from refcode OCERUK onwards) gives structural data for other solvates of *cis*-[M(bpy)$_2$X$_2$] as well as *cis*-[Ru(bpy)$_2$Cl$_2$]·1.7I$_2$, which exhibit the packing motif shown in Figure 7a. Although Nag et al. [42] commented that the unit cell volume increases from 2245(5) Å^3 to 2594(5) Å^3 upon going from *cis*-[Ru(bpy)$_2$Cl$_2$]·3.5H$_2$O (CSD refcode DOGMOB [4]) to *cis*-[Ru(bpy)$_2$Cl$_2$]·1.7I$_2$ (CSD refcode OCERUK [42]), they did not note the similarity of the packing motifs. As in *cis*-[Ru(bpy)$_2$Cl$_2$]·3.5H$_2$O, the [Ru(bpy)$_2$Cl$_2$] molecules in *cis*-[Ru(bpy)$_2$Cl$_2$]·1.7I$_2$ assemble into chains (analogous to that in Figure 7b) with bpy...bpy π-stacking and CH$_{bpy}$...X interactions involving H3 (Table 6). The parameters in Table 6 and the overlaid structures in Figure 8 illustrate the greater offset of the bpy...bpy π-stacking interaction in *cis*-[Ru(bpy)$_2$Cl$_2$]·1.7I$_2$ (red in Figure 8) versus *cis*-[Ru(bpy)$_2$Cl$_2$]·3.5H$_2$O (blue in Figure 8). Nonetheless, the motifs are essentially the same, and 1D-chains similar to that shown in Figure 7b are observed in both compounds. Similar motifs and 1D-chain assembly are found in *cis*-[Ni(bpy)$_2$Br$_2$]·2DMF (DMF = *N*,*N*-dimethylformamide, CSD refcode NIGTEF [44]) except, here, the bpy ligands are crystallographically independent, giving rise to two distinct bpy...bpy π-stacking motifs (Table 6). The same is true in *cis*-[Mn(bpy)$_2$Cl$_2$]·0.5bpy·2.5H$_2$O (CSD refcode XURZOZ [11]) (Table 6) and it is interesting to note that the presence of the free bpy molecules does not disrupt the assembly of packing domains. The compounds *cis*-[Ni(bpy)$_2$Cl$_2$]·MeOH (CSD refcode ABUWAV [48]) and [Os(bpy)$_2$Cl$_2$]·MeOH (CSD refcode CIBJIJ [49]) also exhibit centrosymmetric dimeric motifs similar to that in Figure 7a (Table 6), but hydrogen bonding between the chlorido ligands and MeOH significantly affects the extended packing. In contrast, the introduction of thiourea molecules into the crystal lattice of *cis*-[Mn(bpy)$_2$Cl$_2$]·SC(NH$_2$)$_2$ (CSD refcode ADEVIP) has a significant influence, as detailed by Choudhury et al. [12]. The centrosymmetric dimeric unit found in [Mn(bpy)$_2$Cl$_2$]·SC(NH$_2$)$_2$ (Figure 9) bears a resemblance to motifs described earlier. It involves bpy H4...Cl contacts (Figure 9) and face-to-face π-stacking between only two pyridine rings (centroid...centroid = 3.76 Å), and closely resembles the motif displayed in Figure 5a.

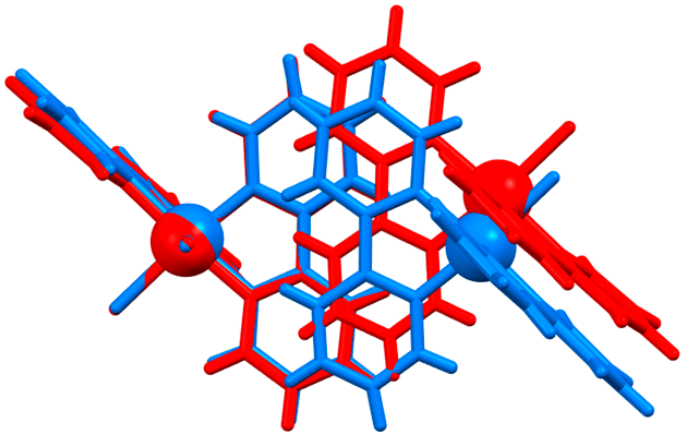

Figure 8. Overlay of the dimeric units in *cis*-[Ru(bpy)$_2$Cl$_2$]·3.5H$_2$O (CSD refcode DOGMOB [4]) shown in blue and in *cis*-[Ru(bpy)$_2$Cl$_2$]·1.7I$_2$ (CSD refcode OCERUK [42]) displayed in red. The molecules on the left are overlaid using pairs of Ru and Cl atoms in Mercury [23]. This reveals the greater offset nature of the bpy...bpy π-stacking interaction in *cis*-[Ru(bpy)$_2$Cl$_2$]·1.7I$_2$ (red) versus *cis*-[Ru(bpy)$_2$Cl$_2$]·3.5H$_2$O (blue).

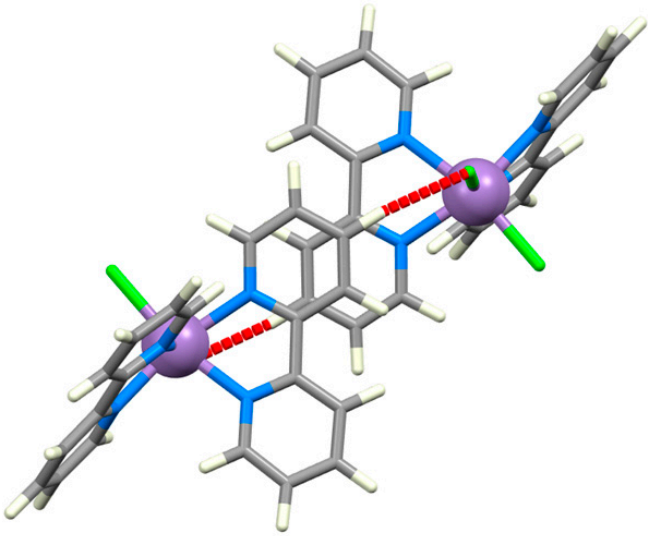

Figure 9. Centrosymmetric packing motif in $[Mn(bpy)_2Cl_2]\cdot SC(NH_2)_2$ (CSD refcode ADEVIP) [12]. The H4...Cl contacts are shown in red (CH4...Cl = 2.591 Å, C...Cl = 3.649(7) Å, angle C–H4...Cl = 163.5°).

In *cis*-$[Co(bpy)_2Cl_2]\cdot 1.5(1,2\text{-}C_2Cl_2H_4)$ (CSD refcode DUYWEZ) [43], the bpy ligands are crystallographically independent. Only one bpy engages in intermolecular π-stacking, leaving the centrosymmetric dimer as the dominant packing motif. The same motif appears in *cis*-$[Ru(bpy)_2Cl_2]\cdot CHCl_3\cdot H_2O$ (CSD refcode AZAQUO) [45], and extends to chains analogous to that depicted in Figure 7b. Two crystallographically independent bpy ligands lead to two distinct centrosymmetric stacking domains. However, as the parameters in Table 6 show, the centroid...centroid distances are long, indicating very weak bpy...bpy π-stacking, and the CH_{bpy}...Cl contacts involving the H3 and H3′ atoms are dominant. The same is true of *cis*-$[Ru(bpy)_2Cl_2]\cdot 2CH_2Cl_2$ (CSD refcodes KESKEP and JEMKEU, Table 6) [46,47]. Note that an orthorhombic polymorph of *cis*-$[Ru(bpy)_2Cl_2]\cdot 2CH_2Cl_2$ (CSD refcode KIJYEI [50]) shows no bpy...bpy face-to-face π-stacking. Molecules of the complex pack in heterochiral layers with the CH_2Cl_2 molecules embraced by four *cis*-$[Ru(bpy)_2Cl_2]$ molecules; the motif is supported by bpy H3...$Cl_{solvate}$ (CH...Cl = 3.020 Å, C...Cl = 3.675(4) Å, angle C–H...Cl = 119.1°) and bpy H4...$Cl_{complex}$ (CH...Cl = 2.971 Å, C...Cl = 3.881(3) Å, angle C–H...Cl = 141.2°) contacts, as shown in Figure 10.

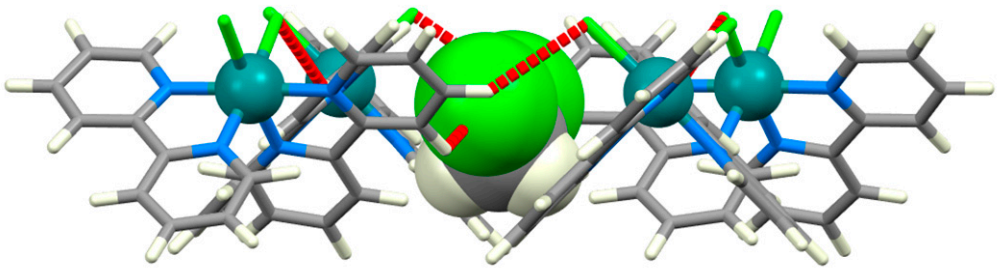

Figure 10. Encapsulation of a CH_2Cl_2 molecule in the orthorhombic polymorph of *cis*-$[Ru(bpy)_2Cl_2]\cdot 2CH_2Cl_2$ (CSD refcode KIJYEI [50]); bpy H3...$Cl_{solvate}$ and bpy H4...$Cl_{complex}$ contacts are shown in red.

The hydrate *cis*-$[Cd(bpy)_2F_2]\cdot 3.5H_2O$ (CSD refcode YAYMET) [6] is the only example of a bis(2,2′-bipyridine)difluoridometal(II) complex, and the crystal structure consists of heterochiral layers of *cis*-$[Cd(bpy)_2F_2]$ molecules separated by sheets of hydrogen-bonded water molecules. The compound crystallizes in the triclinic space group $P\overline{1}$ with two independent *cis*-$[Cd(bpy)_2F_2]$ molecules in the asymmetric unit. The structure exhibits two

crystallographically independent, but similar, centrosymmetric bpy...bpy π-stacking units (Figure 11a) with centroid...centroid distances of 3.65 and 3.66 Å, respectively, as described by Kruszynski [6]. Although this unit bears a resemblance to that in Figure 7a, the bpy H3 atoms in *cis*-[Cd(bpy)$_2$F$_2$]·3.5H$_2$O form CH$_{bpy}$...F contacts with adjacent molecules (Table 7) and the motif shown in Figure 11b is completed by intermolecular F...F contacts, which were discussed in the original work [6].

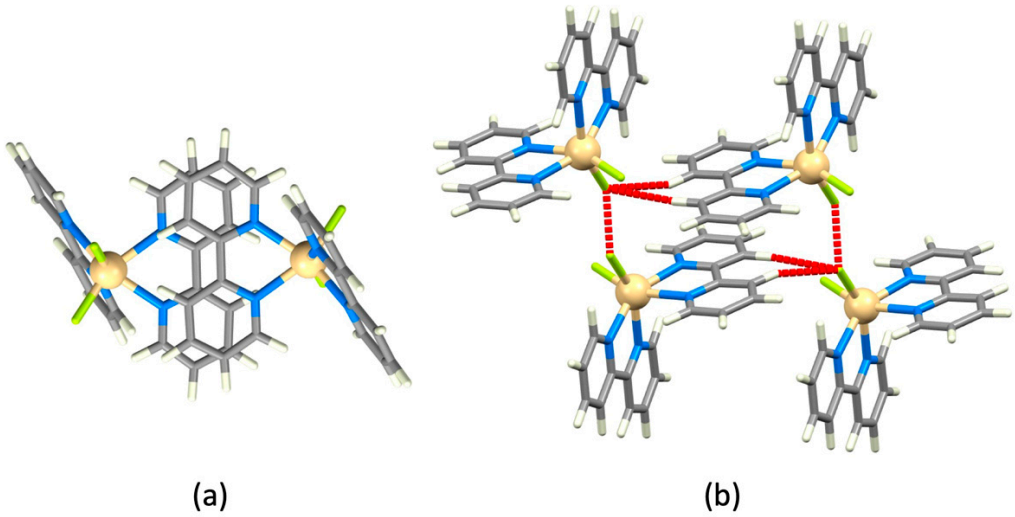

Figure 11. (**a**) One of two crystallographically independent centrosymmetric bpy...bpy π-stacking motifs in *cis*-[Cd(bpy)$_2$F$_2$]·3.5H$_2$O (CSD refcode YAYMET) [6]. (**b**) The bpy H3 and H3′ atoms in the motif shown in (**a**) form CH...F interactions with adjacent molecules; H...F and F...F contacts are shown in red. In the second crystallographically independent motif of this type, only one H...F distance is short enough to be considered (see Table 7).

Table 7. Metric parameters for CH...F short contacts in *cis*-[Cd(bpy)$_2$F$_2$] (Figure 6) involving bpy H3 and H3′ atoms (see Figure 8b). There are two crystallographically independent but similar motifs.

REFCODE Space Group	M	X	CH...X/Å	C...X/Å	∠C–H...X/°	Ref
YAYMET $P\overline{1}$	Cd	F	2.511, 2.733, 2.618	3.559(7), 3.816(8), 3.618(9)	161.0, 172.8, 152.4	[6]

Of the 21 solvated *cis*-[M(bpy)$_2$X$_2$] compounds, only three fail to exhibit a dimeric motif supported by intermolecular CH$_{bpy}$...X and bpy...bpy π-stacking interactions. These are *cis*-[Os(bpy)$_2$Cl$_2$]·CH$_2$Cl$_2$ (CSD refcode UKOHOT [51]), *cis*-[Fe(bpy)$_2$Cl$_2$]·MeCO$_2$Me (CSD refcode HAJGAB [52]), and *cis*-[Ni(bpy)$_2$Cl$_2$]·2DMF (CSD refcode PORKIQ, PORKIQ01 [53]). The latter two compounds are structurally similar and comprise heterochiral layers separated by sheets of methyl acetate or DMF molecules.

6. Conclusions

Following from our observations of dominant crystal-packing motifs in the solid-state structures of [M(bpy)$_3$]$^{q+}$ salts containing halide, [XY$_3$]$^{m-}$ or [XY$_4$]$^{m-}$ anions [2,3], we now draw attention to persistent supramolecular motifs in the solid-state structures of [M(bpy)$_2$X$_2$] complexes with M = any metal and X = F, Cl, Br, and I. The crystal structures of non-solvated *cis*-[M(bpy)$_2$X$_2$] compounds exhibit a ubiquitous motif supported by CH$_{bpy}$...X (X = Cl, Br, I) interactions (CH$_{bpy}$ = H3, H4 or H5) and a bpy...bpy π-stacking interaction. For the dominant group of compounds that crystallize in the monoclinic space group $P2_1/c$, the data in Table 2 illustrate that longer M–X bonds lead to less efficient π-stacking contact, and alternative packing arrangements emerge that mostly retain a

π-stacked motif supported by H3/4/5...X interactions. In solvated *cis*-[M(bpy)$_2$X$_2$] compounds, the dimeric motif supported by intermolecular CH$_{bpy}$...X and bpy...bpy π-stacking interactions is again prevalent. The only fluorido complex in the *cis*-[M(bpy)$_2$X$_2$ family is *cis*-[Cd(bpy)$_2$F$_2$]·3.5H$_2$O and this also exhibits dimeric bpy...bpy π-stacked units; however, CH$_{bpy}$...F contacts involve additional molecules.

The identification of the dimeric motif supported by CH$_{bpy}$...X and bpy...bpy π-stacking interactions and associated with some of the commonest ligands (halides and oligopyridines) potentially adds an additional and valuable tool to the arsenal available for designed crystal engineering.

Author Contributions: The authors contributed equally to the writing of this work. Conceptualization: E.C.C. and C.E.H. Data mining and evaluation: E.C.C. and C.E.H. All authors have read and agreed to the published version of the manuscript.

Funding: This research received no external funding.

Data Availability Statement: Not applicable.

Acknowledgments: We thank the University of Basel for support.

Conflicts of Interest: The authors declare no conflict of interest.

Sample Availability: Not applicable.

References

1. Groom, C.R.; Bruno, I.J.; Lightfoot, M.P.; Ward, S.C. The Cambridge Structural Database. *Acta Crystallogr. Sect. B Struct. Sci. Cryst. Eng. Mater.* **2016**, *B72*, 171–179. [CrossRef]
2. Constable, E.C.; Housecroft, C.E. Halide Ion Embraces in Tris(2,2′-bipyridine)metal Complexes. *Crystals* **2020**, *10*, 671. [CrossRef]
3. Constable, E.C.; Housecroft, C.E. Embracing $[XY_3]^{m-}$ and $[XY_4]^{m-}$ anions in salts of $[M(bpy)_3]^{q+}$. *Crystals* **2023**, *13*, 97. [CrossRef]
4. Eggleston, D.S.; Goldsby, K.A.; Hodgson, D.J.; Meyer, T.J. Structural Variations Induced by Changes in Oxidation State and Their Role in Electron Transfer. Crystal and Molecular Structures of *cis*-[Ru(bpy)$_2$Cl$_2$]·3.5H$_2$O and *cis*-[Ru(bpy)$_2$Cl$_2$]Cl·2H$_2$O. *Inorg. Chem.* **1985**, *24*, 4573–4584. [CrossRef]
5. McCann, S.; McCann, M.; Casey, M.T.; Jackman, M.; Devereux, M.; McKee, V. Syntheses and X-ray crystal structures of *cis*-[Mn(bipy)$_2$Cl$_2$]·2H$_2$O·EtOH and *cis*-[Mn(phen)$_2$Cl$_2$] (bipy = 2,2′-bipyridine; phen = 1,10-phenanthroline); catalysts for the disproportionation of hydrogen peroxide. *Inorg. Chim. Acta* **1998**, *279*, 24–29. [CrossRef]
6. Swiatkowski, M.; Kruszynski, R. Revealing the structural chemistry of the group 12 halide coordination compounds with 2,2′-bipyridine and 1,10-phenanthroline. *J. Coord. Chem.* **2017**, *70*, 642–675. [CrossRef]
7. Toyama, M. Crystal Structure of *cis*-Bis(2,2′-bipyridine)dichlorocobalt(III) Nitrate Methanol Solvate. *X-ray Struct. Anal. Online* **2018**, *34*, 41–43. [CrossRef]
8. Hwang, I.-C.; Ha, K. Crystal structure of bis(2,2′-bipyridine-*N,N*′)dibromomanganese(II), MnBr$_2$(C$_{10}$H$_8$N$_2$)$_2$. *Z. Kristallogr. New Cryst. Struct.* **2007**, *222*, 209–210. [CrossRef]
9. Kavitha, S.J.; Panchanatheswaran, K.; Low, J.N.; Glidewell, C. Racemic *cis*-bis(2,2′-bipyridyl)difluorovanadium(III) tetrafluoroborate. *Acta Crystallogr. Sect. E Struct. Rep. Online* **2005**, *E61*, m1965–m1967. [CrossRef]
10. Yamaguchi-Terasaki, Y.; Fujihara, T.; Nagasawa, A.; Kaizaki, S. *cis*-Bis(2,2′-bipyridine)difluorochromium(III) perchlorate. *Acta Crystallogr. Sect. E Struct. Rep. Online* **2007**, *E63*, m593–m595. [CrossRef]
11. Li, Z.; Xu, D.; Nie, J.; Wu, Z.; Wu, J.; Chiang, M.Y. Synthesis and Crystal Structure of Bis(2,2′-Bipyridine-*N,N*′)Dichloromanganese(II) Complex with Free 2,2′-Bipyridine. *J. Coord. Chem.* **2002**, *55*, 1155–1160. [CrossRef]
12. Choudhury, S.R.; Dutta, A.; Mukhopadhyay, S.; Lu, L.-P.; Zhu, M.-L. *cis*-(2,2′-Bipyridyl)dichloromanganese(II)–thiourea (1/1). *Acta Crystallogr. Sect. E Struct. Rep. Online* **2006**, *E62*, m1489–m1491. [CrossRef]
13. Ferbinteanu, M.; Cimpoesu, F.; Andruh, M.; Rochon, F.D. Solid-state chemistry of [Ni(AA)$_3$][PdCl$_4$]·*n*H$_2$O complexes (AA = bipy, phen) and crystal structures of *cis*-diaqua-bis(phenanthroline)nickel(II) tetrachlorozincate and *cis*-dichlorobis(bipyridine)nickel(II). *Polyhedron* **1998**, *17*, 3671–3679. [CrossRef]
14. Ha, K. A second monoclinic polymorph of bis(2,2′-bipyridine-κ^2*N,N*′)diiodidomanganese(II). *Acta Crystallogr. Sect. E Struct. Rep. Online* **2011**, *E67*, m1351. [CrossRef]
15. Kim, N.-H.; Hwang, I.-C.; Ha, K. Bis(2,2′-bipyridine-κ^2*N,N*′)dichloridoplatinum(IV) dichloride monohydrate. *Acta Crystallogr. Sect. E Struct. Rep. Online* **2009**, *E65*, m180. [CrossRef]
16. Lumme, P.O.; Lindell, E. Structure of *cis*-Bis(2,2′-bipyridine-*N,N*′)dichloromanganese(II). *Acta Crystallogr. Sect. C Cryst. Struct. Commun.* **1988**, *C44*, 463–465. [CrossRef]
17. Prajapati, R.; Yadav, V.K.; Dubey, S.K.; Durham, B.; Mishra, L. Reactivity of metal (Zn^{II}, Ru^{II})-2,2′-bipyridyl with some bifunctional ligands. *Ind. J. Chem.* **2008**, *47A*, 1780–1786.

18. Čechová, D.; Martišková, A.; Moncol, J. Structure of *cis*-dichlorobis(1,10-phenanthroline)manganese(II) and *cis*-dichlorobis(2,2′-bipyridine)manganese(II). *Acta Chim. Slovaca* **2014**, *7*, 15–19. [CrossRef]
19. Fischer, E.; Hummel, H.-U. Untersuchungen im quasi-binären System LiI/2,2′-Bipyridin. *Z. Anorg. Allg. Chem.* **1997**, *623*, 483–486. [CrossRef]
20. Wojciechowska, A.; Bronowska, W.; Pietraszko, A.; Staszak, Z.; Cieślak-Golonka, M. Synthesis, crystal structure and spectroscopic characterisation of double salt $[Zn(bpy)_3](CrO_4)_{0.5}NO_3 \cdot 6.5H_2O$. *J. Mol. Struct.* **2002**, *608*, 151–160. [CrossRef]
21. Chesnut, D.J.; Haushalter, R.C.; Zubieta, J. The hydrothermal synthesis and structural characterization of a new class of compounds: Nickel organoamine-halocadmates. *Inorg. Chim. Acta* **1999**, *292*, 41–51. [CrossRef]
22. Bruno, I.J.; Cole, J.C.; Edgington, P.R.; Kessler, M.; Macrae, C.F.; McCabe, P.; Pearson, J.; Taylor, R. New software for searching the Cambridge Structural Database and visualising crystal structures. *Acta Crystallogr. Sect. B Struct. Crystallogr. Cryst. Chem.* **2002**, *B58*, 389–397. [CrossRef] [PubMed]
23. Macrae, C.F.; Sovago, I.; Cottrell, S.J.; Galek, P.T.A.; McCabe, P.; Pidcock, E.; Platings, M.; Shields, G.P.; Stevens, J.S.; Towler, M.; et al. Mercury 4.0: From visualization to analysis, design and prediction. *J. Appl. Crystallogr.* **2020**, *53*, 226–235. [CrossRef] [PubMed]
24. Miloserdov, F.M.; Kirillova, M.S.; Muratore, M.E.; Echavarren, A.M. Unified Total Synthesis of Pyrroloazocine Indole Alkaloids Sheds Light on Their Biosynthetic Relationship. *J. Am. Chem. Soc.* **2018**, *140*, 5393–5400. [CrossRef] [PubMed]
25. Janiak, C. A critical account on π–π stacking in metal complexes with aromatic nitrogen-containing ligands. *J. Chem. Soc. Dalton Trans.* **2000**, 3885–3896. [CrossRef]
26. Ha, K. Crystal structure of bis(2,2′-bipyridine-*N,N′*)diiodomanganese(II), $MnI_2(C_{10}H_8N_2)_2$. *Z. Kristallogr. New Cryst. Struct.* **2011**, *226*, 187–188. [CrossRef]
27. Park, H.-M.; Hwang, I.-H.; Bae, J.-M.; Jo, Y.-D.; Kim, C.; Kim, H.-Y.; Kim, Y.-M.; Kim, S.-J. Anion Effects on Crystal Structures of Cd^{II} Complexes Containing 2,2′-Bipyridine: Photoluminescence and Catalytic Reactivity. *Bull. Korean Chem. Soc.* **2012**, *33*, 1517–1522. [CrossRef]
28. Skelton, B.W.; Waters, A.F.; White, A.H. Synthesis and Structural Systematics of Nitrogen Base Adducts of Group 2 Salts. VII: Some Complexes of Group 2 Metal Halides with Aromatic *N,N′*-Bidentate Ligands. *Aust. J. Chem.* **1996**, *49*, 99–115. [CrossRef]
29. Ruiz, A.C.; Damodaran, K.K.; Suman, S.G. Towards a selective synthetic route for cobalt amino acid complexes and their application in ring opening polymerization of *rac*-lactide. *RSC Adv.* **2021**, *11*, 16326–16338. [CrossRef]
30. Gao, S.; Ng, S.W. Bis(2,2′-bipyridine-κ^2*N,N′*)dichloridocadmium(II). *Acta Crystallogr. Sect. E Struct. Rep. Online* **2010**, *E66*, m1692. [CrossRef]
31. Zhang, B.-S. Bis(2,2′-bipyridine-κ^2*N,N′*)dibromidocadmium(II). *Acta Crystallogr. Sect. E Struct. Rep. Online* **2009**, *E65*, m1413. [CrossRef] [PubMed]
32. Shirley, H.; Parkin, S.; Delcamp, J.H. Photoinduced Generation of a Durable Thermal Proton Reduction Catalyst with in Situ Conversion of $Mn(bpy)(CO)_3Br$ to $Mn(bpy)_2Br_2$. *Inorg. Chem.* **2020**, *59*, 11266–11272. [CrossRef] [PubMed]
33. Yang, E.-L.; Zhang, N.; Shan, Z.-M.; Wang, Y.-L.; Hu, H.-C.; Liu, Q.-Y. Ionothermal Syntheses and Crystal Structures of Two Cobalt(II) Compounds: $Co(2,2'\text{-bpy})_2Br_2$ and $Co(1,10\text{-phen})_2Br_2$. *Chin. J. Struct. Chem.* **2011**, *30*, 196–201.
34. Dorval, C.; Tricoire, M.; Begouin, J.-M.; Gandon, V.; Gosmini, C. Cobalt-Catalyzed C(sp^2)–CN Bond Activation: Cross-Electrophile Coupling for Biaryl Formation and Mechanistic Insight. *ACS Catal.* **2020**, *10*, 12819–12827. [CrossRef]
35. Guo, H.-X.; Lin, H.-B.; Wang, Q.-H. *cis*-Bis(2,2′-bipyridine)diiodocadmium(II). *Acta Crystallogr. Sect. E Struct. Rep. Online* **2006**, *E62*, m1239–m1240. [CrossRef]
36. Nishio, M. CH/π hydrogen bonds in crystals. *CrystEngComm* **2004**, *6*, 130–158. [CrossRef]
37. Ha, K. Crystal structure of *cis*-bis(2,2′-bipyridine-κ^2*N,N′*)dibromidomanganese(II), $C_{20}H_{16}Br_2MnN_4$. *Z. Kristallogr. New Cryst. Struct.* **2017**, *232*, 149–150. [CrossRef]
38. Zhu, J.-W.; Yang, E.; Song, X.-C.; Lin, Y.-D. Bis(2,2′-bipyridine-κ^2*N,N′*)dibromidocadmium(II). *Acta Crystallogr. Sect. E Struct. Rep. Online* **2007**, *E63*, m1044–m1045. [CrossRef]
39. Muley, A.; Karumban, K.S.; Kumbhakar, S.; Giri, B.; Maji, S. High phenoxazinone synthase activity of two mononuclear *cis*-dichlorocobalt(II) complexes with a rigid pyridyl scaffold. *New J. Chem.* **2021**, *46*, 521–532. [CrossRef]
40. Kumar, K.A.; Amuthaselvi, M.; Dayalan, A. *cis*-Bis(2,2′-bipyridine-κ^2*N,N′*)dichloridocobalt(II) trihydrate. *Acta Crystallogr. Sect. E Struct. Rep. Online* **2011**, *E67*, m468. [CrossRef]
41. Blasberg, F.; Bolte, M.; Wagner, M. *CCDC 2158871: Experimental Crystal Structure Determination*; CCDC: Cambridge, UK, 2022. [CrossRef]
42. Nag, S.; Drew, M.G.B.; Datta, D. Intercalation of diiodine molecules in *cis*-$Ru(bpy)_2Cl_2$. *Inorg. Chem. Commun.* **2006**, *9*, 310–312. [CrossRef]
43. Kramer, T.; Strahle, J. Synthese, Eigenschaften und Struktur von Bipyridin-Halogeno-Komplexen des Cobalts. *Z. Naturforsch.* **1986**, *B41*, 692–696. [CrossRef]
44. Dudkina, Y.B.; Fayzullin, R.R.; Lyssenko, K.A.; Gubaidullin, A.T.; Kholin, K.V.; Levitskaya, A.I.; Balakina, M.Y.; Budnikova, Y.H. Cyclometalated Nickel Complexes as Key Intermediates in C(sp^2)–H Bond Functionalization: Synthesis, Catalysis, Electrochemical Properties, and DFT Calculations. *Organometallics* **2018**, *38*, 1254–1263. [CrossRef]
45. Blasberg, F.; Bolte, M. *CCDC 795576: Experimental Crystal Structure Determination*; CCDC: Cambridge, UK, 2010. [CrossRef]
46. Florke, U.; Ortmeyer, J. *CCDC 1587638: Experimental Crystal Structure Determination*; CCDC: Cambridge, UK, 2017. [CrossRef]

47. Florke, U. *CCDC 1581275: Experimental Crystal Structure Determination*; CCDC: Cambridge, UK, 2017. [CrossRef]
48. Fontaine, F.G. *cis*-Bis(2,2-bipyridine)dichloronickel(II) methanol solvate. *Acta Crystallogr. Sect. E Struct. Rep. Online* **2001**, *E51*, m270–m271. [CrossRef]
49. Yu, M.; Wang, Y.; Hu, J.-M. Synthesis, Crystal Structure and Spectroscopy Studies on Complex *cis*-$Os^{II}(bpy)_2Cl_2$ and Its Oxidation Product [*cis*-$Os^{III}(bpy)_2Cl_2$](PF_6). *Chin. J. Struct. Chem.* **2018**, *37*, 995–1003. [CrossRef]
50. Al-Noaimi, M.; Haddad, S.F. *cis*-Bis(2,2′-bipyridyl)dichloridoruthenium(II) dichloromethane solvate. *Acta Crystallogr. Sect. E Struct. Rep. Online* **2007**, *E63*, m2332. [CrossRef]
51. Groppi, J.; Bartlett, P.N.; Kilburn, J.D. Toward the Control of the Creation of Mixed Monolayers on Glassy Carbon Surfaces by Amine Oxidation. *Chem. Eur. J.* **2016**, *22*, 1030–1036. [CrossRef]
52. Parsons, S.; Winpenny, R.; Wood, P.A. *CCDC 248214: Experimental Crystal Structure Determination*; CCDC: Cambridge, UK, 2004. [CrossRef]
53. Hipler, B.; Doring, M.; Dubs, C.; Görls, H.; Hübler, T.; Uhlig, E. Bildung und Strukturen von Nickelacyclen des Typs (LL′) $NiCH_2CH_2C(O)O$. *Z. Anorg. Allg. Chem.* **1998**, *624*, 1329–1335. [CrossRef]